Volume Measurement

René G. Aarnink
University Hospital Nijmegen
Hessel Wijkstra

For simple geometric shapes, volume measurements can be performed analytically by measuring the dimensions of the object in question and using the appropriate formula for that shape. Volume formulae are found in geometry and calculus textbooks as well as in reference books such as CRC Press's *Handbook of Mathematical Science* or other references.

Volume can also be measured by fluid displacement. The object whose volume is to be measured is placed in a container filled with fluid and the initial and final volumes are measured. The object's volume is equal to the final volume minus the initial volume. This technique is especially useful for irregularly shaped objects.

Fluids can also be used to measure volume of cavities within objects by filling the cavity entirely with a fluid and then measuring the volume of the fluid after it is removed from the cavity.

The remainder of this chapter is dedicated to the more specific problem of volume measurements in medical applications.

Quantitative volume information can be of importance to the clinician in the diagnosis of a variety of diseases or abnormalities. It can also improve the understanding of the physiology of the patient. Information on volume may be used in various applications such as cardiac monitoring, diagnosis of prostate diseases, follow-up during organ transplantation, surgery for tumor resection, blood flow measurements, plastic surgery, follow-up of preterm infants, sports performance analysis, etc. Because of this wide spectrum of applications, various techniques for volume measurements have been developed, some of which are useful in determining the amount of blood flow to the organ (dynamic), while others are used to obtain the size of the object (static). The techniques can be invasive or noninvasive, and are based on either direct or indirect measurements. Each technique has its own advantages and disadvantages, and the application determines the selection of volume measurement method.

One of the earliest techniques to measure (changes of) body volume was *plethysmography*, originally developed by Glisson (1622) and Swammerdam (1737) to demonstrate isovolumetric contraction of isolated muscle. The measuring technique consists of surrounding the organ or tissue with a rigid box filled with water or air. The displacement of the fluid or the change in air pressure indicates the volume

changes of the tissue due to arterial in-flow. Two major types of plethysmography exist, and these can be distinguished by the technique used to measure the volume change. These are *volume plethysmography* (direct-measurement displacement plethysmography including water and air types), and *electrical plethysmography* (strain-gages, inductive and impedance plethysmographs). The physical condition in which the measurements should be performed determines the plethysmographic method chosen.

Advances in medical imaging have provided new possibilities for noninvasively extracting quantitatively useful diagnostic information. Images are constructed on a grid of small picture elements (pixels) that reflect the intensity of the image in the array occupied by the pixel. Most medical images represent a two-dimensional projection of a three-dimensional object.

Currently, the most commonly used medical imaging modalities are ultrasound, nuclear magnetic resonance imaging, X-rays and X-ray computer tomography. *Ultrasound imaging* is based on the transmission and reflection of high-frequency acoustic waves. Waves whose frequencies lie well above the hearing range can be transmitted through biological tissue and will be reflected if they cross a boundary between media of different acoustic properties. These reflected signals can be reconverted to electrical signals and displayed to obtain a two-dimensional section. *Magnetic resonance imaging* is based on the involvement of the interaction between magnetic moment (or spin) of nuclei and a magnetic field. The proton spins are excited by an external radio frequency signal and the return to an equilibrium distribution is used to construct cross-sectional images. *Computer tomography* or *CT-scanning* uses a rotating source of X-rays. The X-ray source and detector are scanned across a section of the object of interest, and the transmission measurements are used to reconstruct an image of the object.

These imaging techniques display cross-sections of views that can be used to estimate the size of specific components. One way to estimate the volume of internal objects is make certain assumptions concerning the shape and to apply formulae to estimate the volume with dimensions of the object such as length, height, and width. A more accurate technique is *step-section planimetry*, a clinical application of numerical integration. During this procedure, cross-sections of the object are recorded with a certain (fixed) interval. The area of the object is determined in every section, and the total volume is calculated by multiplying the contribution of each section with the interval and summarizing all contributions.

The volume of a fluid-filled region can be calculated if a known quantity of indicator is added to the fluid and the concentration measured after it has been dispersed uniformly throughout the fluid. The selection of the indicator used to measure the volume depends on the application and can be based on temperature, color, or radioactivity.

Finally, volume (changes) can also be performed directly using *water-displacement volumetry*, a sensitive but time-consuming method to measure the volume of an extremity. This method is not suitable for patients in the immediate postoperative period.

13.1 Plethysmography Theory

Fluid in-flow can be measured by blocking the out-flow and then measuring the change in volume due to the in-flow over a defined time interval. Plethysmography enables the volume change to be determined in a reasonably accurate manner. A direct-volume displacement plethysmograph uses a rigid chamber usually filled with water, into which the limb or limb segment is placed. This type of plethysmograph, sometimes called *chamber plethysmography*, can be used in two ways. It can be used to measure the sequence of pulsations proportional to the individual volume changes with each heart beat (arterial plethysmography or rheography). Also, the total amount of blood flowing into the limb or digit can be measured by venous occlusion: by inflating the occluding cuff placed upstream of the limb or digit just above the venous pressure 5 kPa to 8 kPa (40 mm Hg to 60 mm Hg), arterial blood can enter the region but venous blood is unable to leave. The result is that the limb or digit increases its volume with each heart beat by the volume entering during that beat.

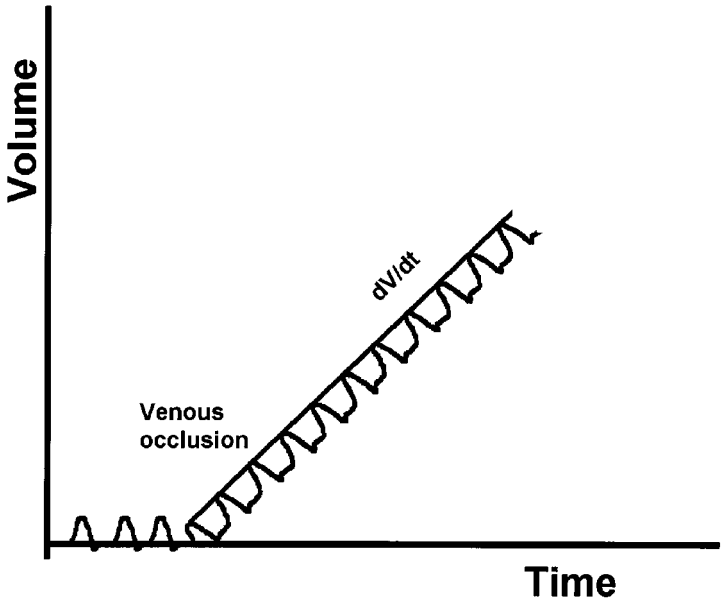

FIGURE 13.1 Typical recording from air plethysmograph during venous occlusion, revealing the changes in volume over time caused by arterial in-flow.

Air/Water Plethysmography or Chamber Plethysmography

Air plethysmography uses the relation between the volume change of a gas in a closed system and the corresponding pressure and temperature [1]. The relation between pressure and volume is described by Boyle's law, which can be written as:

$$P_i V_i = P_f V_f \tag{13.1}$$

with P_i and V_i the initial pressure and volume, respectively, and P_f and V_f the final pressure and volume, measured at constant temperature: the displacement of the fluid or the compressing of the air is a direct measure of the blood flow or original volume. The air plethysmograph uses the change in pressure that occurs in a cuff wrapped around the segment of interest due to the change in volume. By inflating the cuff to about 60 mm Hg, the arterial in-flow causes small increases in pressure. These small changes in pressure over the cardiac cycle can be monitored (see Figure 13.1). The measurement of blood flow is achieved by comparing the pressure changes to changes caused by removing known amounts of air from the system. The second measurement uses volume changes at various pressures between systolic and diastolic pressures, and the peak deflection is compared with the deflection caused by removal of known amounts of air from the system. In segmental plethysmography, two cuffs are used to measure the volume changes in a segment of a limb. Venous occlusion is established by the first cuff, while the second is inflated to a pressure that will exclude blood flow from those parts that should not be included in the measurement.

The technique can also be used for whole-body plethysmography [2], a common technique used to measure residual volume, functional residual capacity (FRC), and total lung volume, the parameters usually determined during pulmonary function testing [3]. In body plethysmography, the patient sits inside an airtight box, and inhales or exhales to a particular volume (usually the functional residual capacity, the volume that remains after a normal exhalation). Then, a shutter closes the breathing tube,

while the subject tries to breathe through the closed tube. This causes the chest volume to expand and decompress the air in the lungs. The increase in chest volume slightly reduces the air volume of the box, thereby increasing the pressure. First, the change in volume of the chest is quantified using Boyle's law with the initial pressure and volume of the box, and the pressure in the box after expansion. The change in volume of the box is equal to the change in volume of the chest. A second measurement using the initial volume of the chest (unknown) and the initial pressure at the mouth, and the inspiratory volume (the unknown chest volume and the change in volume obtained in the first measurement) together with the pressure at the mouth during the inspiratory effort. By solving Boyle's law for the unknown volume, the original volume of gas present in the lungs when the shutter was closed is obtained, which is normally the volume present at the end of a normal exhalation or FRC.

Alternative methods for measurement of volume changes with plethysmography have been introduced to overcome the disadvantages of chamber plethysmography such as cost, complexity, and awkwardness of use. Important alternatives are elastic-resistance strain-gage plethysmography, impedance plethysmography, inductive plethysmography, and photoelectric plethysmography.

Electrical Plethysmography

Strain-Gage Plethysmography

In 1953, Whitney described the elastic-resistance strain-gage plethysmograph [4]. The strain-gage instrument quantifies the change in resistance of the gage as it is stretched due to the enlargement of the object (e.g., limb segment). The gage is typically a small elastic tube filled with mercury or an electrolyte or conductive paste. The ends of the tube are sealed with copper plugs or electrodes that make contact with the conductive column. These plugs are connected to a Wheatstone bridge circuit.

To illustrate the principle of the strain-gage method, a strain-gage of length l_0 is placed around the limb segment, a circular cross section with radius r_0. The length of the strain-gage can thus also be expressed as $l_0 = 2\pi r_0$. Expansion of the limb gives a new length $l_1 = 2\pi r_1$, with r_1 the new radius of the limb. The increase in length of the strain-gage is thus $\delta l = 2\pi(r_1 - r_0)$, while the change in cross-sectional area of the limb δA is $\pi(r_1^2 - r_0^2)$. This can also be expressed as:

$$\delta A = \pi\left[2r_0\left(r_1 - r_0\right) + \left(r_1 - r_0\right)^2\right] \tag{13.2}$$

Since $r_1 - r_0$ is usually small, $(r_1 - r_0)^2$ can be neglected. Consequently, δA can be written as $2\pi r_0(r_1 - r_0)$ which, on dividing by $A = \pi(r_0)^2$, gives:

$$\frac{\delta A}{A} = 2\frac{r_1 - r_0}{r_0} \tag{13.3}$$

But since $\delta V/V = \delta A/A$ and $\delta l/l = \delta r/r$:

$$\frac{\delta V}{V} = 2\frac{l_1 - l_0}{l_0} \tag{13.4}$$

Thus, the percentage increase in volume can be obtained by measuring the initial gage length and the change in length. In practice, this change in length of the strain-gage is recorded over a relatively short period to overcome the problem of back pressure that builds up in the limb or digit because of the venous occlusion, and the measurement is usually expressed as milliliters per minute per 100 g of tissue, or: volume flow rate = $2(\delta l/l_0) \times (100/t)$, where δl is the increase in gage length during time t. To measure $\delta l/t$, the gage must be calibrated by removing it from the limb and stretching it on a measuring jig until

the pen recorder returns to the zero level; this is the length l_0. The gage can then be stretched accurately by typical amounts, to calibrate the output and calculate the volume flow rate.

Impedance Plethysmography

The physical principle of impedance plethysmography is the variation in electrical impedance of a tissue segment over the cardiac cycle due to a changing conductance. The change is caused by arterial in-flow to the segment while the venous drainage is occluded.

If a segment of limb is assumed to be cylindrical and of length l and volume V, the impedance Z of that part can be written as:

$$Z = \frac{\rho l^2}{V} \tag{13.5}$$

with ρ the specific resistivity of the tissue forming the cylinder.

Blood entering the tissue segment during the cardiac cycle introduces a parallel impedance Z_b described as $Z_b = Z_0 Z_1 / (Z_0 - Z_1)$, with Z_0 the initial impedance and Z_1 the new value. A small change in volume δV is related to a small change in resistance δZ, such that:

$$\delta Z = Z_0 - Z_1 = \rho l^2 \left(\frac{1}{V_0} - \frac{1}{V_1} \right) = \rho l^2 \frac{\left(V_1 - V_0 \right)}{V_1 V_0} \approx -\rho l^2 \frac{\delta V}{V^2} = -Z \frac{\delta V}{V} \tag{13.6}$$

when very small changes in volume are assumed [5]. Thus, δV can be written as:

$$\delta V = \rho \left(\frac{1}{Z_0^2} \right) \delta Z \tag{13.7}$$

and these parameters Z_0 and δZ can be obtained from the impedance plethysmogram. If it is assumed that $\rho = 150\ \Omega$ cm, being the specific resistivity of soft tissue, the change in volume can be determined.

Two major techniques have been used to measure tissue impedance. One method uses two electrodes to measure both the voltage drop across the electrodes and the current flow. The main disadvantage of this technique is that the current distribution in the vicinity of the electrodes is not known, meaning the exact volume of the interrogated tissue is also unknown. In 1974, Kubicek et al. [6] described the use of four electrodes to measure tissue impedance: the outer electrodes supply a small-amplitude, high-frequency ac signal, while the inner two are used to measure the potential difference between two points on the same surface (see Figures 13.2 and 13.3).

Inductive Plethysmography

For measurement of volume changes during respiration, a system based on inductive plethysmography has been developed; the respiratory inductive plethysmograph was introduced in 1978. During inductive plethysmography, two coils are attached — one placed around the rib cage and the other around the abdomen. During respiration, the cross-sectional diameter of the coils changes, leading to a change in the inductances of the coils. By converting these inductances into proportional voltages, a measure for the changes in volume during respiration can be obtained. The conversion is achieved by using oscillators whose frequencies depend on a fixed internal capacitor and the inductance of each coil. These oscillator frequencies are converted to proportional voltages, voltages that are then recorded. After calibration on the patient, the system can be used for respiratory volume measurement [9].

Two general methods have been introduced for calibration of the respiratory inductive plethysmograph. These calibration methods are based on the following equation:

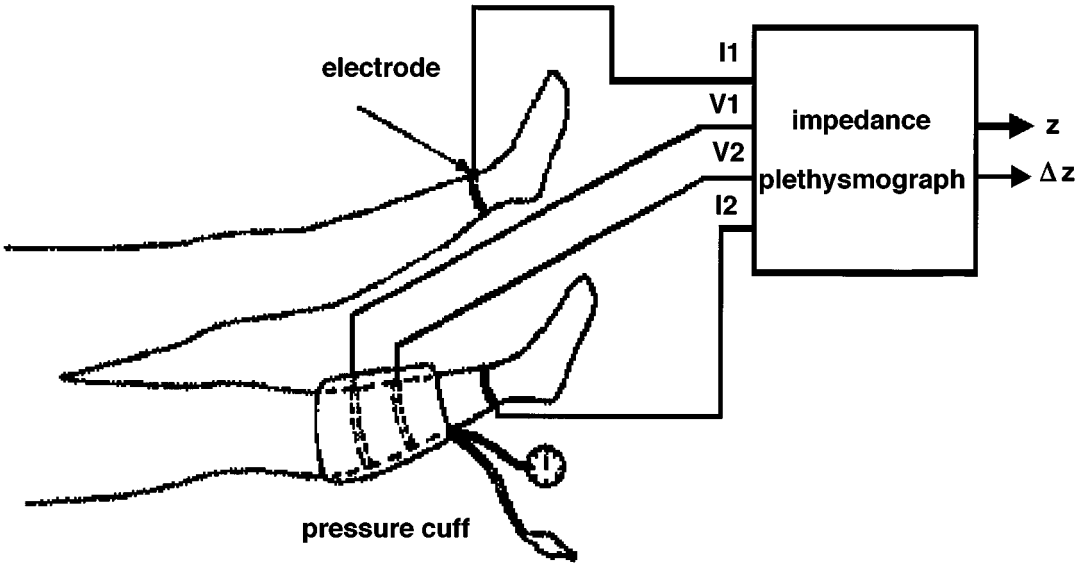

FIGURE 13.2 Electrode positioning for impedance plethysmography used for early detection of peripheral atherosclerosis: the outer two supply current while the inner two measure voltage. The combination of these two is used to obtain the changes in impedance, and these changes are then used to obtain the changes in volume of the leg. (From R. Shankar and J. G. Webster, *IEEE Trans. Biomed. Eng.*, 38, 62-67, 1993. With permission.)

$$V_T = V_{RC} + V_{AB} \tag{13.8}$$

with V_{RC} and V_{AB} the contributions of the rib cage (RC) and abdominal compartments (AB) to the tidal volume V_T. Calibration can be performed by determining the calibration constant in an isovolume measurement or by regression methods of differences in inductance changes due to a different body position or a different state of sleep [10]. Once it is calibrated, the respiratory inductive plethysmograph can be used for noninvasive monitoring of changes of thoracic volume and respiratory patterns.

13.2 Numerical Integration with Imaging

For diagnostic purposes in health care, a number of imaging modalities are currently in use (see also Chapter 79 on medical imaging). Webb nicely reviewed the scientific basis and physical principles of medical imaging [11].

With medical imaging modalities, diameters of objects can be determined in a noninvasive manner. By applying these diameters in an appropriate formula for volume calculation, the size of the object can be estimated. For example, in a clinical setting, the prostate volume V_p can be approximated with an ellipsoid volume calculation:

$$V_p = \frac{\pi}{6} H W L \tag{13.9}$$

with H the height, W the width, and L the length of the prostate as illustrated in Figure 13.4. Variations have been introduced to find the best formulae to estimate the prostate volume [12, 13]. Also, for the determination of ventricular volumes, formulae have been derived, based on the following variation of

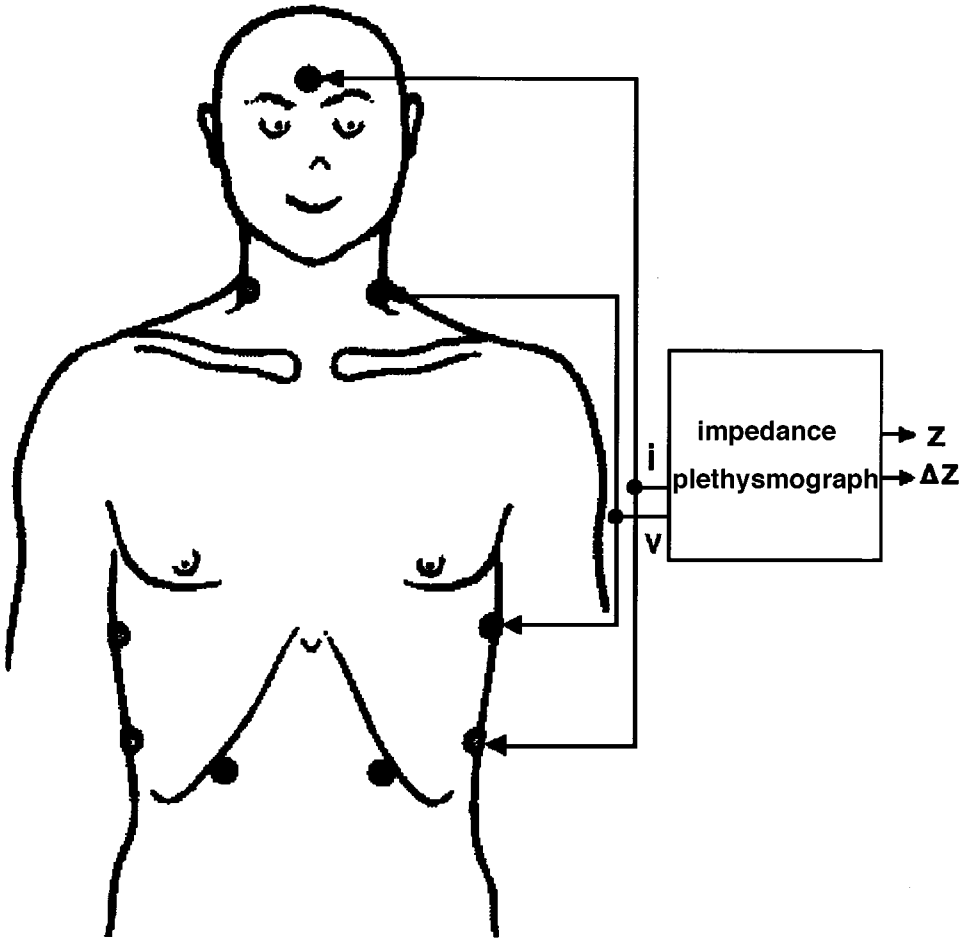

FIGURE 13.3 A second example of electrode positioning for impedance plethysmography, here used to estimate stroke volume: the outer two supply current while the inner two measure voltage. (From N. Verschoor et al., *Physiol. Meas.,* 17, 29-35, 1996. With permission.)

the formula for prostate volume measurements: (1) the volume is obtained with the same formula as for prostate volume measurements, (2) the two short axes are equal, (3) the long axis is twice the short axis, and (4) the internal diameter is used for all axes.

By displaying cross-sectional images of a 3-D object (e.g., an organ), volume calculations can also be performed by integrating areas of the organ over a sequence of medical images as illustrated in Figure 13.5. For ultrasound images, applications have been reported in the literature on prostate, heart, bladder, and kidney volume. The application of integration techniques involves the application of segmentation algorithms on sequences of images, either in transverse direction with fixed intersection distance or in the radial with images at a fixed intersection angle.

For a volume defined by the function $f(x,y,z)$, the volume can be calculated from:

$$V = \int_{x=x_1}^{x_2} \int_{y=y_1}^{y_2} \int_{z=z_1}^{z_2} f(x,y,z)\,\mathrm{d}z\,\mathrm{d}y\,\mathrm{d}x \tag{13.10}$$

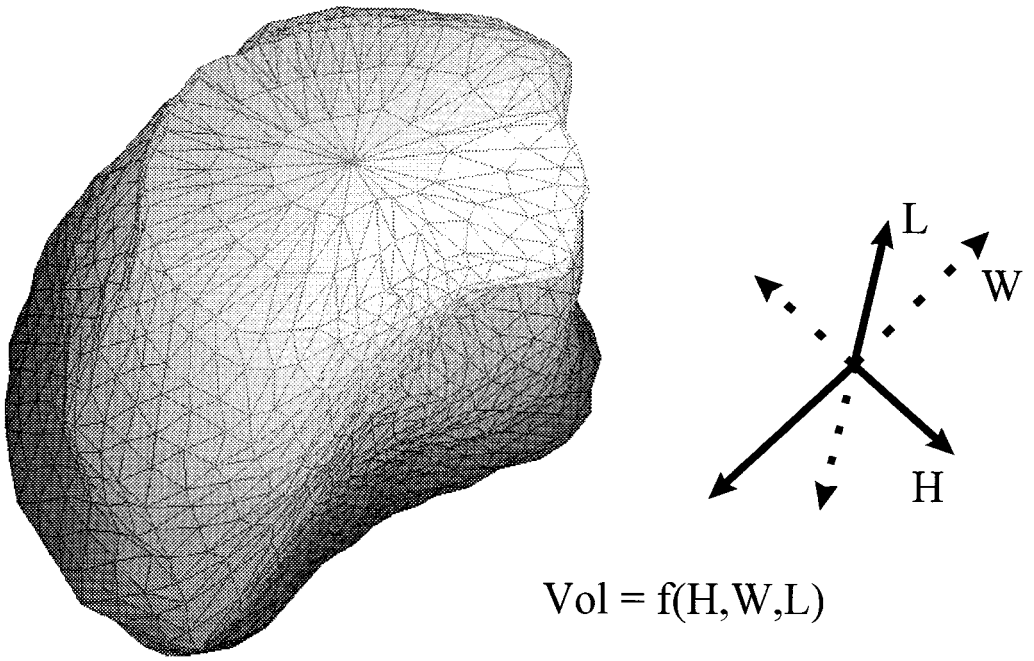

FIGURE 13.4 Volume estimate of a prostate, obtained from 3-D reconstruction of cross-sectional images, using the dimensions in three planes: the length, height, and width in a volume formula describing an ellipsoid shape.

By applying numerical integration, the volume calculation using an integral is approximated by a linear combination of the values of the integrand. For reasons of simplicity, this approximation is first illustrated for a one-dimensional case:

$$\int_{x=a}^{b} f\left(x\right)\mathrm{d}x \approx w_1 f\left(x_1\right) + w_2 f\left(x_2\right) + \ldots + w_{\mathrm{nf}} f\left(x_{\mathrm{n}}\right) \tag{13.11}$$

In this equation, $x_1, x_2, \ldots, x_{\mathrm{n}}$ are n points chosen in the interval of integration $[a,b]$, and the numbers $w_1, w_2, \ldots, w_{\mathrm{n}}$ are n weights corresponding to these points. This approximation can also be expressed in the so-called Riemann sum:

$$\int_{x=a}^{b} f\left(x\right)\mathrm{d}x \approx w_1 f\left(x_1\right) + w_2 f\left(x_2\right) + \ldots + w_{\mathrm{n}} f\left(x_{\mathrm{n}}\right) = \sum_{\mathrm{i}=1}^{\mathrm{n}} f\left(\xi_{\mathrm{i}}\right)\left(x_{\mathrm{i}} - x_{\mathrm{i-1}}\right) \tag{13.12}$$

For volume calculation, the Riemann sum needs to be extended to a three-dimensional case:

$$V = \int_{x=x_1}^{x_2}\int_{y=y_1}^{y_2}\int_{z=z_1}^{z_2} f\left(x,y,z\right)\mathrm{d}z\mathrm{d}y\mathrm{d}x \approx \sum f\left(p_{\mathrm{ijk}}\right)\left(x_{\mathrm{i+1}} - x_{\mathrm{i}}\right)\left(y_{\mathrm{j+1}} - y_{\mathrm{j}}\right)\left(z_{\mathrm{k+1}} - z_{\mathrm{k}}\right) \tag{13.13}$$

This three-dimensional case can be reduced by assuming that $(x_{\mathrm{i+1}} - x_{\mathrm{i}})(y_{\mathrm{i+1}} - y_{\mathrm{i}})f(p_{\mathrm{ijk}})$ represents the surface S_{k} of a two-dimensional section at position z_{k}, while $(z_{\mathrm{k+1}} - z_{\mathrm{k}})$ is constant for every k and equals h, the intersection distance:

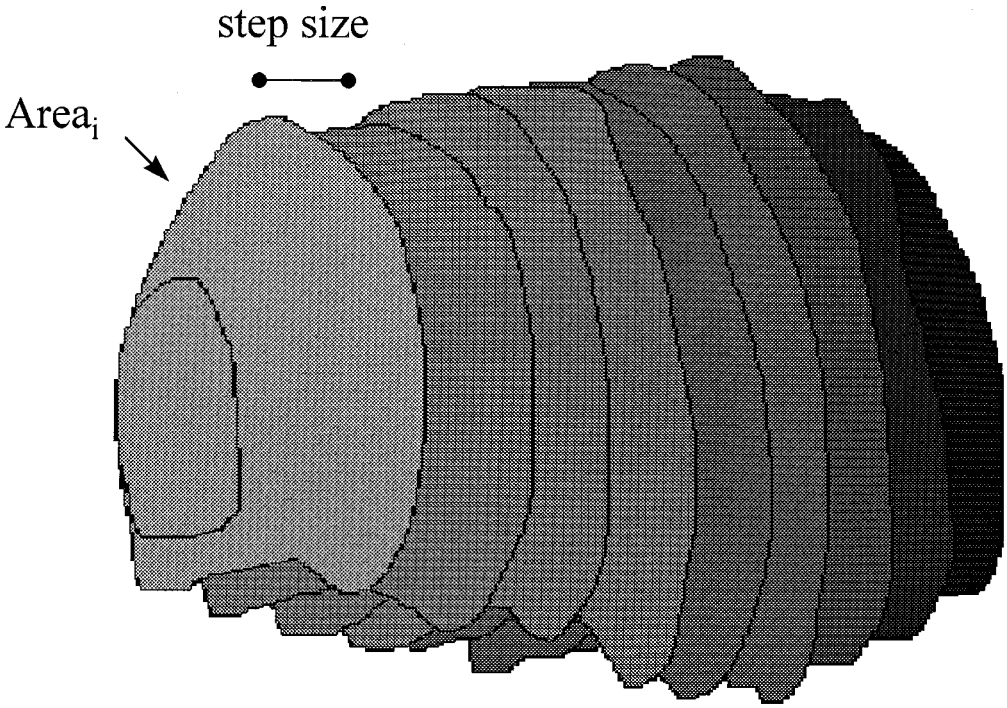

FIGURE 13.5 Outlines of cross-sectional images of the prostate used for planimetric volumetry of the prostate: transverse cross-sections obtained with a step size of 4 mm have been outlined by an expert observer, and the contribution of each section to the total volume is obtained by determining the area enclosed by the prostate contour. The volume is then determined by summarizing all contributions after multiplying them with the step size.

$$V \approx h \sum S\left(z_k\right) = h \sum_{k=0}^{n-1} S\left(a + kh\right) \tag{13.14}$$

where a represents the position of the first section, n the number of sections, and h the step size, given by $h = (b - a)/n$, where b the position of the last section.

In general, three different forms of the approximation can be described, depending on the position of the section. The first form is known as the rectangular rule, and is presented in Equation 13.14. The midpoint rule is described by:

$$V \approx h \sum S\left(z_k\right) = h \sum_{k=0}^{n-1} S\left[a + \left(k + \frac{1}{2}h\right)\right] \tag{13.15}$$

The trapezoidal rule is similar to the rectangular rule, except that it uses the average of the right-hand and left-hand Riemann sum:

$$T_n\left(f\right) = h\left[\frac{f\left(a\right)}{2} + f\left(a+h\right) + f\left(a+2h\right) + \ldots + f\left(a+\left(n-1\right)h\right) + \frac{f\left(b\right)}{2}\right] \tag{13.16}$$

The trapezoidal and midpoint rules are exact for a linear function and converge at least as fast as n^{-2}, if the integrand has a continuous second derivative [14].

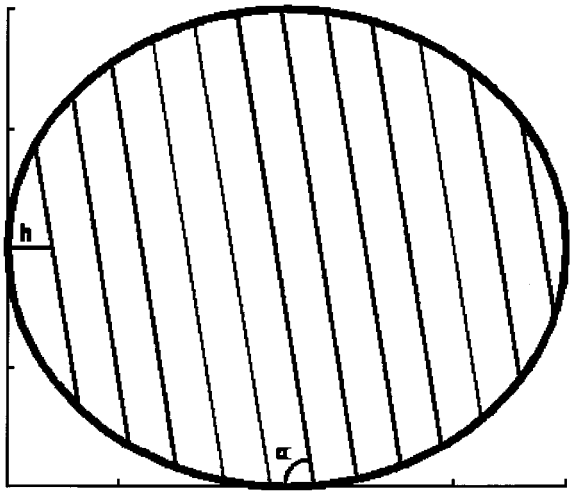

FIGURE 13.6 An ellipsoid-shaped model of the prostate that was used for theoretical analysis of planimetric volumetry. Indicated are the intersection distance *h* and the scan angle α with the axis of the probe. (From R. G. Aarnink et al., *Physiol. Meas.,* 16, 141-150, 1995. With permission.)

A number of parameters are associated with the accuracy of the approximation of the volume integral with a Riemann sum; first of all, the number of cross sections *n* is important as the sum converges with n^{-2}: the more sections, the more accurate the results. Furthermore, the selection of the position of the first section is important. While the interval of integration is mostly well defined in theoretical analyses, for *in vivo* measurements, the first section is often less well defined. This means not only that the selection of this first section is random with the first possible section and this section increased with the step size, but also that sections can be missed. The last effect that may influence the numerical results is the effect of taking oblique sections, cross sections that are not taken perpendicular to the axis along which the intersection distance is measured. All the above assumes that every section S_k can be exactly determined.

The influence of the parameters associated with these kinds of measurements can be tested in a theoretical model. In a mathematical model with known exact volume or surface, the parameters — including step size, selection of the first section, and the scan angle — can be tested. Figure 13.6 shows a model used to model the prostate in two dimensions. It consists of a spheroid function with a length of the long axis of 50 mm and a length of the short axis of 40 mm. In mathematical form, this function can be described as:

$$y = f(x) = y_m \pm y_o \sqrt{1 - \left(\frac{x - x_m}{x_o}\right)^2} \tag{13.17}$$

with x_0 half the diameter of the ellipse in *x*-direction (25 mm) and y_0 half the diameter of the ellipse in *y*-direction (20 mm) and (x_m, y_m) the center point of the ellipse. The analytical solution of the integral to obtain the surface of this model is $\pi x_0 y_0$.

Figure 13.6 also reveals the possible influence of the parameters *h* and α. Figure 13.7 shows the results for varying the step size *h* between 4 mm and 16 mm corresponding to between 13 and 3 sections used for numerical integration as a function of the position of the first section. The first section is selected (at random) between the first coordinate of the function, and this coordinate plus the step size *h*. The sections were taken perpendicular to the long axis. From this study, which is fully described by Aarnink et al. [15], it was concluded that if the ratio of step size to the longest diameter is 6 or more, then the

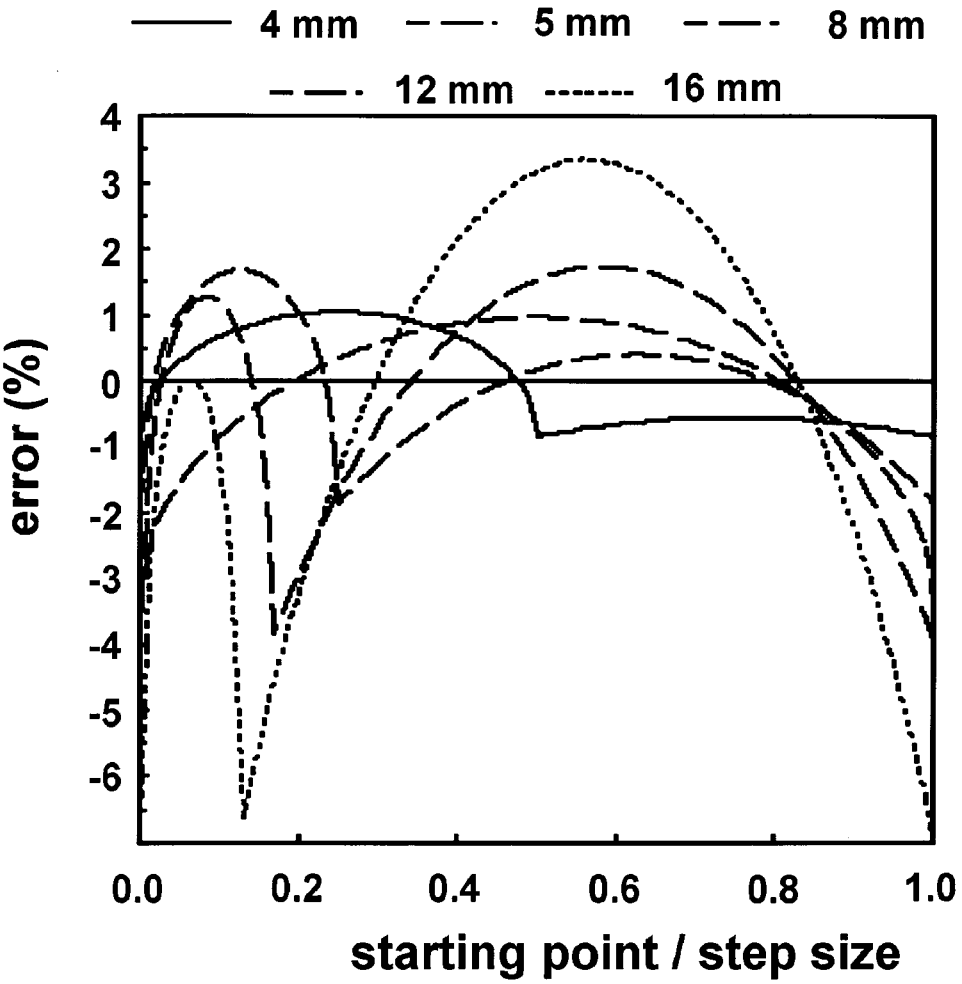

FIGURE 13.7 The errors in surface estimates by numerical integration for different step sizes h presented as percentage of the exact solution, as a function of the position of the first section, located between 0 and h. (From R. G. Aarnink et al., *Physiol. Meas.,* 16, 141-150, 1995. With permission.)

error in volume estimation is less than 5%. Although clinical application might introduce additional errors such as movement artifacts, this rule provides a good indication of the intersection distance that should be used for good approximations with numerical integration.

13.3 Indicator Dilution Methods

The principle of the indicator dilution theory to determine gas or fluid volume was originally developed by Stewart and Hamilton. It is based on the following concept: if the concentration of an indicator that is uniformly dispersed in an unknown volume is determined, and the volume of the indicator is known, the unknown volume can be determined. Assuming a single in-flow and single out-flow model, all input will eventually emerge through the output channel, and the volumetric flow rate can be used to identify the volume flow. It can be described with two equations, of which the second is used to determine the volume using the result of the first equation [16]:

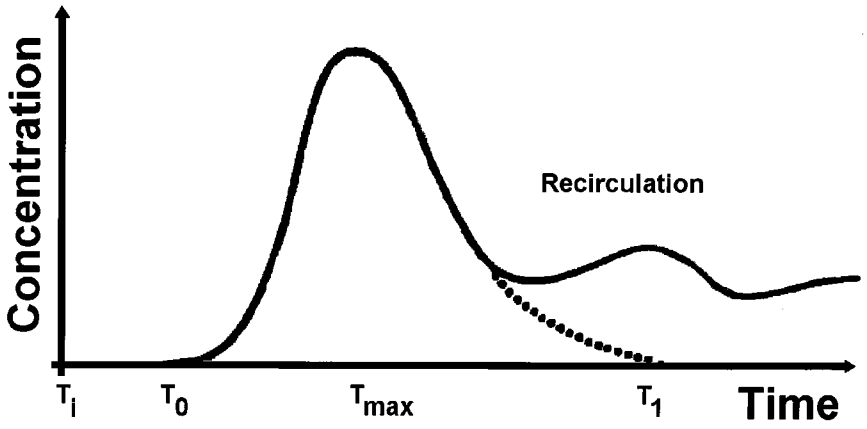

FIGURE 13.8 The time-concentration curve of the indicator is used to obtain the unknown volume of the fluid. The area under the time-concentration curve is needed to estimate the volumetric flow rate, and this flow rate can be used to estimate the volume flow. For accurate determination of the flow rate, it is necessary to extrapolate the first pass response before the area under the curve is estimated.

$$F = \frac{I_i}{\int_0^\infty C(t)\,dt} \tag{13.18}$$

$$\text{Volume} = F\, t_m \tag{13.19}$$

where F = flow rate
I_i = total quantity of injected indicator
$C(t)$ = concentration of the contrast as function of time
Vol = volume flow
t_m = mean transit time

The integrated value of the concentration over time can be obtained from the concentration-time curve (Figure 13.8) using planimetry and an approximation described by the Riemann sum expression (Equation 13.13). Care must be taken to remove the influence of the effect of recirculation of the indicator. An indicator is suitable for use in the dilution method if it can be detected and measured, and remains within the circulation during at least its first circuit, without doing harm to the object. Subsequent removal from the circulation is an advantage. Dyes such as Coomassie blue and indocyanine green were initially used, using the peak spectral absorption at certain wavelengths to detect the indicator. Also, radioisotopes such as I-labeled human serum albumin have been used. Currently, the use of cooled saline has become routine in measurement of cardiac output in the intensive care unit.

Thermodilution

To perform cardiac output measurements, a cold bolus (with a temperature gradient of at least 10E) is injected into the right atrium and the resulting change in temperature of the blood in the pulmonary artery is detected using a rapidly responding thermistor. After recording the temperature-time curve, the blood flow is calculated using a modified Stewart-Hamilton equation. This equation can be described as follows [17]:

$$V_i\ SW_i\ SH_i\left(T_b - T_i\right) = F\int T_b\left(dt\right) SW_b\ SH_b \tag{13.20}$$

The terms on the left represent the cooling of the blood (with temperature T_b), as caused by the injection of a cold bolus with volume V_i, with temperature T_i, specific weight SW_i and specific heat SH_i. The same amount of "indicator" must appear in the blood (with specific weight and heat SW_b and SH_b, respectively) downstream to the point of injection, where it is detected in terms of the time-course of the temperature T_b in the flow F by means of a thermistor. The flow can be described as:

$$F = \frac{T_b - T_i}{\int T_b\left(dt\right)} K \tag{13.21}$$

where K (the so-called calculation constant) is described as:

$$K = V_i \frac{SW_i - SH_i}{SW_b - SH_b} C \tag{13.22}$$

This constant is introduced to the computer by the user. T_i is usually measured at the proximal end of the injection line; therefore, a "correction factor" C must be introduced to correct for the estimated losses of cold saline in the catheter, due to the dead space volume. Furthermore, the warming effect of the injected fluid during passing through the blood must be corrected; this warming effect depends on the speed of injection, the length of immersion of the catheter, and the temperature gradient. This warming effect reduces the actual amount of injected fluid, so the correction factor C is less than 1 [17].

Radionuclide Techniques

Radionuclide imaging is a common noninvasive technique used in the evaluation of cardiac function and disease. It can be compared to X-ray radiology, but now the radiation emanating from inside the human body is used to construct the image. Radionuclide imaging has proven useful to obtain ejection fraction and left ventricular volume. As in thermodilution, a small volume of indicator is injected peripherally; in this case, radioisotopes (normally indicated as radiopharmaceuticals) are used. The radioactive decay of radioisotopes leads to the emission of alpha, beta, gamma, and X radiation, depending on the radionuclide used. For *in vivo* imaging, only gamma- or X-radiation can be detected with detectors external to the body, while the minimal amount of energy of the emitted photons should be greater than 50 keV. Using a photon counter such as a Gamma camera, equipped with a collimator, the radioactivity can be recorded. Two techniques are commonly used: the first pass method and the dynamic recording method [11].

First Pass Method

To inject a radionuclide bolus into the blood system, a catheter is inserted in a vein, for example, an external jugular or an antecubital vein. The camera used to detect the radioactive bolus is usually positioned in the left anterior oblique position to obtain optimal right and left ventricular separation, and is tilted slightly in an attempt to separate left atrial activity from that of the left ventricle. First, the background radiation is obtained by counting the background emissions. Then, a region of interest is determined over the left ventricle and a time-activity curve is generated by counting the photon emissions over time. The radioactivity count over time usually reveals peaks at different moments; the first peak occurs when the radioactivity in the right ventricle is counted, the second peak is attributed to left ventricular activity. More peaks can occur during recirculation of the radioactivity. After correction for

background emissions, the time-intensity curve is evaluated to determine the ejection fraction (*EF*) of the heart, which is given by:

$$EF = \frac{c_d - c_s}{c_d - c_b} \tag{13.23}$$

where c_d is the end diastolic count, c_s is the end systolic count, and c_b is the background count [18]. Using a dynamic cardiac phantom, the accuracy of the *EF* measurement and *LV* volume estimation by radionuclide imaging has been determined [18]. The count-based method was found to give accurate results for evaluating cardiac *EF* and volume measurements.

Dynamic Recording Method

During dynamic recording, the data acquisition is triggered by another signal, usually the ECG, to obtain the gated activity during ventricular systole and diastole. The contraction of the left ventricle of the heart is used to align the acquisition data from different cardiac cycles. During dynamic recording, information about the cardiac function is averaged over many heart beats during a period when the radiopharmaceuticals are uniformly distributed in the blood pool. Estimations of end systolic and end diastolic volumes are made and the ejection fraction is calculated (see above). Also, other parameters can be obtained; for example, the amplitude and phase of the ejection from the left ventricle. These parameters may show malfunction in the cardiac cycle. These dynamic recordings may also be applied to the brain, lungs, liver, kidney, and vascular systems and they can be important to judge the function of these organs (e.g., after kidney transplantation).

Gas Dilution

Gas dilution is a method to determine lung volumes because standard techniques for lung measurements measure only the inhaled or exhaled air as a function of time (spirometry) and cannot be used to assess the absolute lung volume. The subject is connected to a spirometer that contains a known concentration of gas (e.g., helium). The subject is then asked to breathe for several minutes, to equalize the concentration of helium in the lung and the spirometer. Using the law of conservation of matter, the volume of the lung can be calculated. Since the total amount of helium is the same before and after measurement, the fractional concentration times the volume before equals the fractional concentration times the volume after: $C_1 \times V_1 = C_2 \times (V_1 + V_2)$. The volume after the measurement can be extracted from this equation and, by subtracting the volume of the spirometer, the lung volume is calculated.

13.4 Water Displacement Volumetry

The measurement of the volume of an extremity such as arm or leg can be measured using a water tank, which is illustrated schematically in Figure 13.9. The advantage of water displacement volumetry is the possibility for direct measurement of objects with an irregular form. In the clinical situation, volume determination of the leg can be valuable for monitoring the severity of edema or hematoma after surgery or trauma. A setup for water displacement can be developed by the user, and an example of such a system is described by Kaulesar Sukul et al. [19]. A special tank for water displacement volumetry of the leg was constructed consisting of two overflow tubes. The tank was filled to the lower overflow tube, and the overflow tube was subsequently closed. The patient was then asked to lower his leg into the tank, and the amount of overflow of the upper tube was measured. The total volume was then calculated by measuring the fluid volume delivered to the upper tube and the volume difference between the lower and upper overflow tube, the so-called "reserve volume." The volume of ankle and foot was then measured by filling the tank to the upper overflow tube and measuring the amount of water in the cylinder when the foot and ankle were immersed in the water.

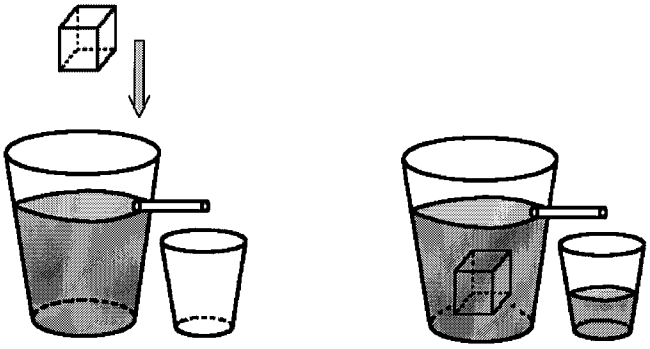

FIGURE 13.9 A schematic overview of a volume measuring method using water displacement: the desired volume of the object is represented by the overflow volume in the small tank after lowering the object into the large tank. This technique is especially useful for irregular-shaped objects.

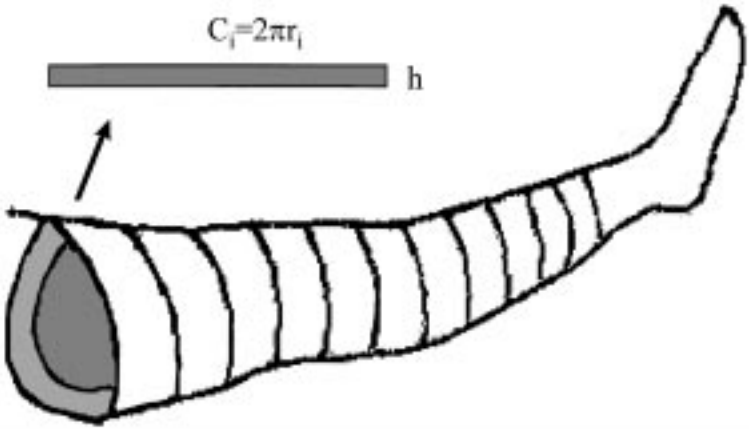

FIGURE 13.10 Illustration of the disk model to measure leg volume. The leg is divided in different sections with a fixed intersection distance the circumference of each section is obtained. This circumference is then used to describe the leg as perfect circles with an assumed radius calculated from the circumference. This radius is then used to calculate the contribution of that section to the volume and the total volume is obtained by summation.

Disadvantages of water displacement volumetry are hygiene problems, it is time-consuming, and not suitable for measurements of the volume of extremities of patients in the immediate postoperative period. Therefore, alternatives have been sought, with the disk model method as a promising one. The calculation of the volume of the leg is performed by dividing the leg into disks of thickness h (e.g., 3 cm) as illustrated in Figure 13.10. The total volume is equal to the sum of the individual disk volumes:

$$V = \sum_{i=1}^{n} \frac{C_i^2}{4\pi} h = \sum_{i=1}^{n} \pi r_i^2 h = h \sum_{i=1}^{n} \pi r_i^2 \tag{13.24}$$

where C_i is the circumference of the disk at position i with assumed radius of r_i.

A study to compare water displacement volumetry with the results of the disk model method indicated that both methods give similar results. Consequently, because of the ease of application, the disk model method is the method of choice to measure volumes of extremities. Assuming the length of a leg to be 75 cm, a ratio between length and step size (3 cm was proposed in [19]) of 25 is obtained. According to

TABLE 13.1 Volume Measuring Techniques, Applications, and Equipment for Different Applications

Technique	Application	Companies	Products	Price (U.S.$)
Spirometry	Lung volume	Nellcor Puritan Bennett	Renaissance	
		Morgan Science		
		Spirometrics		
		CDX Corporation	Spiro 110S	
Whole-body plethysmography	Lung volume	Morgan Science		
		ACI Medical Inc.		25,000.00
Gas-dilution	Lung volume	Equilibrated Biosystems Inc. Melville		
Thermodilution	Heart	Abbott Critical Care System		
		Baxter		
		American Edwards Laboratories		
Strain-gage plethysmography	Cardiac output	Parks Medical Electronics		
Impedance plethysmography	Perfusion studies	Ambulatory monitoring systems		
		Vitalog		
		RJL systems Detroit		
		Codman and Shurtleff Inc. Randolph		
		Electrodiagnostic Instrument Inc. Burbank		
Inductive plethysmograph	Lung volume	SensorMedics BV	RespiTrace plus	
			SomnoStar PT	15,000.00
Radionuclide imaging	Heart, peripheral organs	Schering		

a study by Aarnink et al. [15], this ratio can be reduced while still obtaining an accuracy of >95%. A disk height of 10 cm will be sufficient to measure the leg volume with an accuracy of at least 95%. However, it might be necessary to use a small interdisk section to obtain a higher accuracy, which might be needed to accurately monitor the edema changes in volume.

13.5 Equipment and Experiments

Table 13.1 summarizes the different methods for volume measurement and their applications. The table serves as a starting point to evaluate the available equipment for volume measurement.

13.6 Evaluation

Plethysmography is an easy and noninvasive method to obtain knowledge for assessing vascular diseases, cardiac output disorders, or pulmonary disfunctions. Systems for direct measurement of volume changes have been developed, but physical properties have also been introduced as an indirect measure of the change in volume. Each system has its own advantages and disadvantages.

For *chamber plethysmography*, the water-filled type is more stable with respect to temperature change but thermal problems may occur if the water temperature is significantly different from that of the limb segment. Furthermore, the hydrostatic effect of the water may alter the blood flow. Also, the rubber sleeve between the limb segment and the water may influence the release of sweat. It is a cumbersome measurement that is not very useful during or after exercise. The *air displacement* type introduces problems of drift because of its high coefficient of expansion, although self-compensating systems have been proposed. Also, the thermal behavior of the body plethysmograph may produce variations in pressure inside the airtight box. Two sources of temperature variation can be mentioned: the chest volume

variation induced by breathing produces heat and a temperature gradient may exist between the patient and the internal temperature of the box [20].

In *impedance plethysmography,* the changes in impedance in tissue are used, which are primarily due to changes in the conductivity of the current path with each pulsation of blood. Several theories attempt to explain the actual cause of these changes in tissue impedance. One explanation is that blood-filling of a segment of the body lowers the impedance of that segment. A second theory is that the increase in diameter due to additional blood in a segment of the body increases the cross-sectional area of the segment's conductivity path and thereby lowers the resistance of the path. A third explanation is based on the principle of pressure changes on the electrodes that occur with each blood pulsation and uses the changes in the impedance of the skin–electrode interface. The main difficulty with the procedure is the problem of relating the output resistance to any absolute volume measurement. Detection of the presence of arterial pulsations, measurement of pulse rate, and determination of time of arrival of a pulse at any given point in the peripheral circulation can all be satisfactorily handled by impedance plethysmography. Also, the impedance plethysmograph can measure time-variant changes in blood volume. A problem with impedance plethysmography may be the sensitivity to movement of the object. Research is being conducted to reduce the influences of these movement artifacts, either by different electrode configuration, electrode location, or using multiple sensors or different frequencies [21].

A low-cost *inductive plethysmograph* was designed by Cohen et al. to obtain a noninvasive measure of lung ventilation [22]. This plethysmograph indirectly monitors ventilation by measuring the cross-sectional area of the chest and abdomen. They attached commercially available elastic bands containing wire around the chest and abdomen and determined their inductances by measuring the frequency of an inductive-controlled oscillator.

New devices for plethysmographic measurements are under development, using different properties to obtain the quantitative knowledge required. For example, *acoustic plethysmography* measures body volume by determining changes in the resonant frequency of a Helmholtz resonator. A Helmholtz resonator consists of an enclosed volume of gas connected to its surroundings through a single opening. The gas can be forced to resonate acoustically by imposing periodic pressure fluctuations of the opening. The resonator frequency is inversely proportional to the square root of the volume of air in the resonator. An object placed in the resonator reduces the volume of air remaining in the resonator by its own volume, causing an increase in the resonator frequency. From a study to obtain density values of preterm infants, it was concluded that the acoustic plethysmograph can be used to measure total body volume of preterm infants [23].

In addition, volume measurements with diagnostic imaging modalities are well established in the clinical environment; for example, prostate ultrasonography or echocardiography. Besides important parameters such as step size and first step selection, accurate determination of the surface in different sections is important. While predominantly performed manually now, several attempts for automated detection of the surface have been reported [24–27]. Automatic detection of the surface in each section should be possible and would enable a system for automated measurement of the prostate, heart, liver, etc. Further research will indicate the usefulness of such a system in a clinical setting.

References

1. A. J. Comerota, R. N. Harada, A. R. Eze, and M. L. Katz, Air plethysmography: a clinical review, *Int. Angiology,* 14, 45-52, 1995.
2. A. B. Dubois, S. J. Botello, G. N. Beddell, R. Marshall, and J. H. Comroe, A rapid plethysmographic method for measuring thoracic gas volume: a comparison with a nitrogen washout method for measuring functional residual capacity in normal subjects, *J. Clin. Invest.,* 35, 322-326, 1956.
3. J. B. West, *Respiratory Physiology — The Essentials,* Baltimore, MD: Williams and Wilkins, 1987.
4. J. R. Whitney, The measurement of volume changes in human limbs, *J. Physiol.,* 121, 1-27, 1953.
5. J. Nyboer, S. Bagno, and L. F. Nims, The Impedance Plethysmograph: An Electrical Volume Recorder, National Research Council, Committee on Aviation Medicine, Rep. No. 149, 1943.

6. W. G. Kubicek, F. J. Kottke, M. V. Ramos, R. P. Patterson, D. A. Witsoe, J. W. Labree, W. Remole, T. E. Layman, H. Schoening, and J. T. Garamala, The Minnesota impedance cardiograph — Theory and applications, *Biomed. Eng.,* 9, 410-416, 1974.
7. R. Shankar and J. G. Webster, Noninvasive measurement of compliance of human leg arteries, *IEEE Trans. Biomed. Eng.,* 38, 62-67, 1993.
8. N. Verschoor, H. H. Woltjer, B. J. M. van der Meer, and P. M. J. M. de Vries, The lowering of stroke volume measured by means of impedance cardiography during endexpiratory breath holding, *Physiol. Meas.,* 17, 29-35, 1996.
9. M. A. Cohn, H. Watson, R. Weisshaut, F. Stott, and M. A. Sackner, A transducer for non-invasive monitoring of respiration, in *ISAM 1977, Proc. Sec. Int. Symp. Ambulatory Monitoring*, London: Academic Press, 1978, 119-128.
10. J. A. Adams, Respiratory inductive plethysmography, in J. Stocks, P. D. Sly, R. S. Tepper, and W. J. Morgan (eds.), *Infant Respiratory Function Testing,* New York: Wiley-Liss, 1996, 139-164.
11. S. Webb, *The Physics of Medical Imaging,* Bristol, U.K.: IOP Publishing, 1988, 204-221.
12. M. K. Terris and T. A. Stamey, Determination of prostate volume by transrectal ultrasound, *J. Urol.,* 145, 984-987, 1991.
13. R. G. Aarnink, J. J. M. C. H. de la Rosette, F. M. J. Debruyne, and H. Wijkstra, Formula-derived prostate volume determination, *Eur. Urol.*, 29, 399-402, 1996.
14. P. J. Davis and P. Rabinowitz, *Methods of Numerical Integration*, San Diego: Academic Press, 1975, 40-43.
15. R. G. Aarnink, R. J. B. Giesen, J. J. M. C. H. de la Rosette, A. L. Huynen, F. M. J. Debruyne, and H. Wijkstra, Planimetric volumetry of the prostate: how accurate is it?, *Physiol. Meas.,* 16, 141-150, 1995.
16. E. D. Trautman and R. S. Newbower. The development of indicator-dilution techniques, *IEEE Trans. Biomed. Eng.,* 31, 800-807, 1984.
17. A. Rubini, D. Del Monte, V. Catena, I. Ittar, M. Cesaro, D. Soranzo, G. Rattazzi, and G. L. Alatti, Cardiac output measurement by the thermodilution method: an *in vitro* test of accuracy of three commercially available automatic cardiac output computers, *Intensive Care Med.,* 21, 154-158, 1995.
18. S. Jang, R. J. Jaszczak, F. Li, J. F. Debatin, S. N. Nadel, A. J. Evans, K. L. Greer, and R. E. Coleman, Cardiac ejection fraction and volume measurements using dynamic cardiac phantoms and radionuclide imaging, *IEEE Trans. Nucl. Sci.,* 41, 2845-2849, 1994.
19. D. M. K. S. Kaulesar Sukul, P. T. den Hoed, E. J. Johannes, R. van Dolder, and E. Benda, Direct and indirect methods for the quantification of leg volume: comparison between water displacement volumetry, the disk model method and the frustum sign model method, using the correlation coefficient and the limits of agreement, *J. Biomed. Eng.,* 15, 477-480, 1993.
20. P. Saucez, M. Remy, C. Renotte, and M. Mauroy, Thermal behavior of the constant volume body plethysmograph, *IEEE Trans. Biomed. Eng.,* 42, 269-277, 1995.
21. J. Rosell, K. P. Cohen, and J. G. Webster, Reduction of motion artifacts using a two-frequency impedance plethysmograph and adaptive filtering, *IEEE Trans Biomed. Eng.,* 42, 1044-1048, 1995.
22. K. P. Cohen, D. Panescu, J. H. Booske, J. G. Webster, and W. L. Tompkins, Design of an inductive plethysmograph for ventilation measurement, *Physiol. Meas.,* 15, 217-229, 1994.
23. O. S. Valerio Jimenez, J. K. Moon, C. L. Jensen, F. A. Vohra, and H. P. Sheng, Pre-term infant volume measurements by acoustic plethysmography, *J. Biomed. Eng.,* 15, 91-98, 1993.
24. R. G. Aarnink, R. J. B. Giesen, A. L. Huynen, J. J. M. C. H. de la Rosette, F. M. J. Debruyne, and H. Wijkstra, A practical clinical method for contour determination in ultrasonographic prostate images, *Ultrasound Med. Biol.,* 20, 705-717, 1994.
25. C. H. Chu, E. J. Delp, and A. J. Buda, Detecting left ventricular endocardial and epicardial boundaries by digital two-dimensional echocardiography, *IEEE Trans. Med. Im.,* 7, 81-90 1988.
26. J. Feng, W. C. Lin, and C. T. Chen, Epicardial boundary detection using fuzzy reasoning, *IEEE Trans. Med. Im.,* 10, 187-199, 1991.
27. S. Lobregt and M. A. Viergever, A discrete contour model, *IEEE Trans. Med. Im.,* 14, 12-24, 1995.

Further Information

Anonymous, AARC Clinical Practice Guideline; Static lung volume, *Respir. Care,* 39, 830-836, 1994.
Anonymous, AARC Clinical Practice Guideline; Body plethysmography, *Respir. Care,* 39, 1184-1190, 1994.
E. F. Bernstein (ed.), *Noninvasive Diagnostic Techniques in Vascular Disease,* 3rd ed., St. Louis: Mosby, 1985.
P. J. Davis and P. Rabinowitz, *Methods of Numerical Integration,* London: Academic Press, 1975.
H. Feigenbaum, *Echocardiography,* 5th ed., Philadelphia: Lee & Febiger, 1993.
W. N. McDicken, *Diagnostic Ultrasonics: Principles and Use of Instruments,* 3rd ed., London: Crosby Lockwood Staples, 1991.
J. Nyboer, *Electrical Impedance Plethysmography*, Springfield, IL: Charles Thomas, 1959.
S. Webb, *The Physics of Medical Imaging*, Bristol: IOP Publishing, 1988.
J. B. West, *Respiratory Physiology — The Essentials,* Baltimore, MD: Williams and Wilkins, 1987.